International Journal of
Automotive Manufacturing and Materials (IJAMM)

Scilight

Article

Study on the Influence of Sprocket Tooth Profile Tolerances on Engine NVH

Qi Zhang *, Jie Liu, Xiao Zhang, Wei Zhai, Bo Zhou, and Shihua Li

R&D Center, Dongfeng Automobile Co. Ltd., Wuhan 430074, China
* Correspondence: dfac-zhangqi@dfac.com
Received: 3 September 2025; Revised: 22 December 2025; Accepted: 18 May 2026; Published: 22 June 2026

Abstract: Addressing the thumping noise generated during the operation of diesel engine chain-driven oil pumps, this paper systematically investigates the noise influence mechanism of sprocket tooth chamfer tolerances through theoretical analysis and experimental validation. A meshing impact dynamics model based on Hertzian contact theory reveals how sprocket chamfer dimensions amplify noise energy via the coupled effects of contact stress concentration and system resonance response. Analysis of vehicle NVH test results for oil pumps equipped with sprockets featuring different tooth flank chamfers confirms significant noise characteristics influenced by chamfer dimensions, aligning closely with theoretical predictions. Based on these findings, an optimized sprocket tooth profile tolerance scheme is proposed, resolving abnormal idle noise in the vehicle. This research provides theoretical support and engineering guidance for optimizing NVH performance in engine chain drive mechanisms.

Keywords: diesel engine; chain-driven oil pump; tooth flank chamfering; thumping noise

1. Introduction

In diesel engine transmission systems, gear drives and chain drives are two common drive methods. Gear drives offer advantages such as high stability, high transmission efficiency, and smooth meshing. However, gear meshing tends to generate high-frequency noise, necessitating optimized helical gear designs that increase manufacturing costs. In contrast, chain drives offer high adaptability and lower costs. Yet their complex multibody dynamics, coupled with the polygon effect during chain-sprocket engagement, can induce periodic impact noise.

In recent years, the NVH characteristics of chain drive systems have attracted considerable research attention. Studies on the polygon effect and meshing impact have revealed the fundamental mechanisms of vibration excitation in chain drives [1,2]. Researchers have investigated the influence of chain pitch, sprocket tooth profile geometry, and tensioner dynamics on the overall system response [3,4]. For instance, investigations into the effects of speed fluctuations and load variations have deepened understanding of how operating conditions modulate impact energy [5]. Furthermore, structural path analysis and acoustic holography have been employed to identify noise transmission paths and optimize housing designs for noise attenuation [6–8]. Despite these efforts, a systematic research gap remains concerning the quantitative relationship between sprocket tooth profile micro-geometry—particularly the chamfer dimensions—and the resulting NVH performance, especially in terms of coupled resonance excitation. The innovation of this paper lies in establishing a multiphysics coupling model that links tooth flank chamfer tolerances to radiated noise through the chain of "contact stress–impact energy–resonance response," providing a quantitative optimization methodology for this specific but critical geometric parameter.

As a core component driving both diesel engine timing and oil pumps, the noise level of chain drive systems directly determines the engine's NVH (Noise, Vibration, and Harshness) performance. NVH significantly impacts driving comfort and passenger experience, serving as a key indicator of automotive quality. With the advancement of the automotive industry, NVH has become a focal point for both vehicle manufacturers and component suppliers, holding particular importance in enhancing user satisfaction and brand competitiveness [9,10].

2. Project Background

The subject of this research is a 2.3 L turbocharged diesel engine paired with an automatic transmission. Originally equipped with a gear-driven oil pump system, this engine was later modified to a chain-driven system to enhance lightweighting and reduce manufacturing costs.

During high-altitude testing for a certain project, one of the 20 test vehicles exhibited a thumping noise at warm-up idle (750 rpm). This noise occurred at a frequency of six times per second, closely approximating the half-step frequency of 6.25 Hz (as shown in Figure 1). This phenomenon is directly related to the inherent characteristics of chain drives: compared to the constant meshing behaviour of gear drives, chain drives are prone to periodic impact loads due to polygon effects, and their non-linear vibration characteristics are more readily excited under conditions such as low-speed idling [11,12]. In high-altitude environments, combustion fluctuations caused by thin air may further amplify the impact energy from sprocket-chain meshing, resulting in a perceptible thumping noise [13].

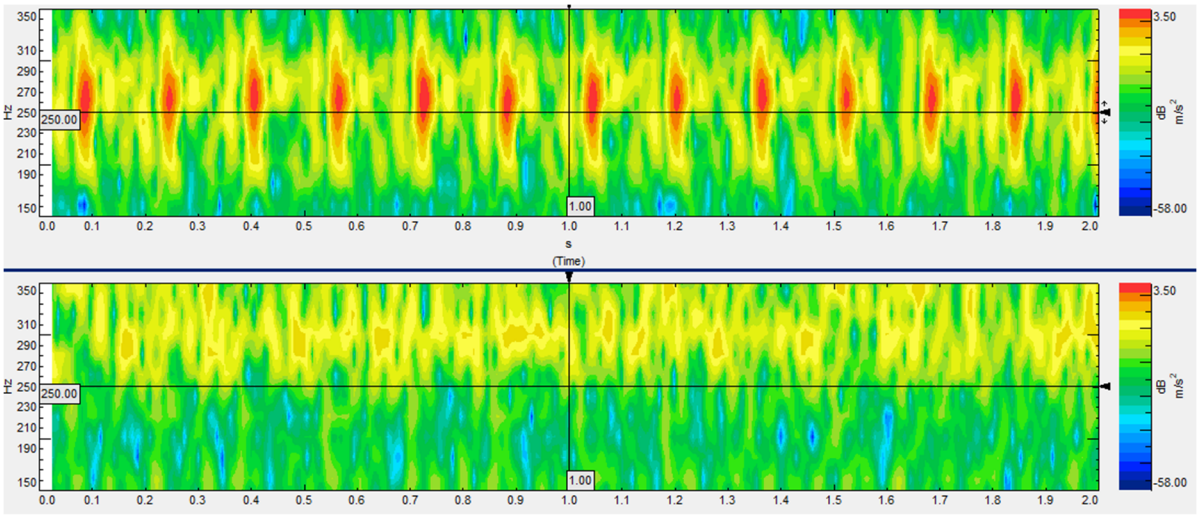

Figure 1. Thumping noise characteristics.

2.1. Noise Source Localization

To identify the origin of the thumping noise, a fault tree analysis (FTA) was conducted on the entire vehicle. By sequentially removing the transmission and torque converter, it was observed that the noise intensity diminished but did not cease entirely. Further analysis revealed that after transmission removal, the overall modal characteristics of the engine and transmission changed, disrupting the resonance frequency. After removing only the torque converter, the noise persisted at a lower level, confirming the transmission was not the source. Subsequently, an engine swap test was performed on the complete vehicle: the knocking sound disappeared after the replacement engine was installed, and reinstalling the original engine caused the sound to reappear. This confirmed that the knocking noise originated from the engine assembly (ABA validation).

2.2. Key Frequency Band Analysis

During motoring testing (engine running without ignition) on the engine test bench, a characteristic noise (6 times per second) was consistently detected, ruling out combustion noise as the primary factor. Further testing at idle speed with an additional 50 N·m torque applied verified the load's impact on mechanical meshing characteristics. The noise knocking intensity significantly increased, indicating that increased load exacerbates impact vibration in moving components [14].

Analysis of near-field noise measurements revealed that noise energy was concentrated in the 200–300 Hz frequency band, with a stable knocking frequency of 6 times per second. This frequency closely matches the engine's half-order operating frequency of 6.25 Hz. Preliminary suspicion points to a modulation effect caused by periodic excitation in the 200–300 Hz band interacting with the 6.25 Hz frequency, leading to periodic amplification of noise intensity [15].

2.3. Part Inspection and Positioning

The simplified diagram of this engine's transmission mechanism is shown in Figure 2. Based on the preceding analysis, we first investigated components operating at the 6.25 Hz half-order frequency. Analysis of the collected noise revealed intermittent vibrations at 270 Hz in the vacuum pump body, occurring six times per second. This frequency is close to the half-order of 6.25 Hz. Furthermore, the vacuum pump has a speed ratio of 0.5 and an order of 0.5, matching the order of the abnormal noise. Verification on the entire vehicle showed that the noise persisted even after removing the vacuum pump, indicating its minor contribution to the noise.

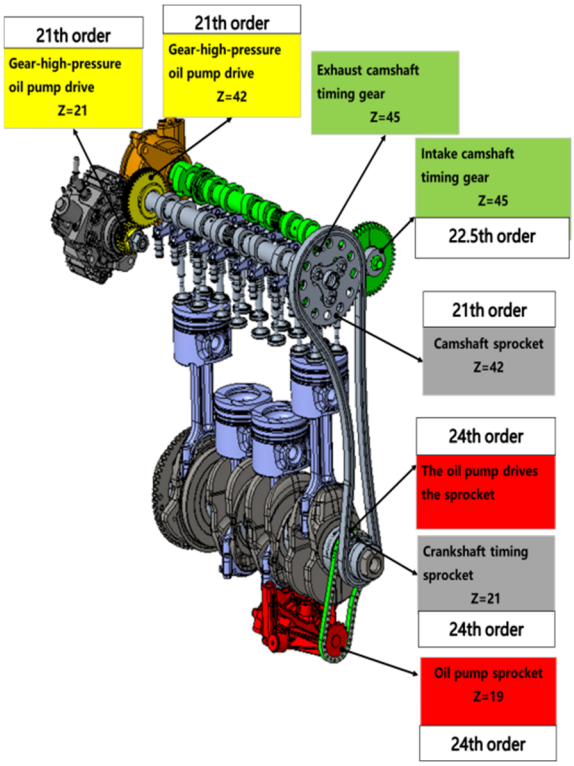

Figure 2. Schematic Diagram of the Internal Transmission Mechanism of the Engine.

Subsequently, based on the engine transmission mechanism schematic, components operating at half-order frequencies were systematically investigated according to internal order sequence (e.g., single-cylinder piston, high-pressure fuel pump, valves, intake camshaft, exhaust camshaft, as listed in Table 1). None of these components produced noticeable noise improvement. The investigation focus was ultimately shifted to components operating in the 200–300 Hz range.

Table 1. Workpiece Inspection Checklist.

Part Name	Order	Effect on Noise	Remarks
Vacuum pump	half-order	No significant impact	non-primary cause
Single-cylinder piston	half-order	No significant impact	non-primary cause
High-pressure oil pump	Piston half-order	No significant impact	non-primary cause
valve	half-order	No significant impact	non-primary cause
Intake camshaft	half-order	No significant impact	non-primary cause
Exhaust camshaft	half-order	No significant impact	non-primary cause

The oil pump sprocket operates at a 24th-order mode. At engine idle, its operating frequency is 300 Hz, overlapping with the characteristic noise frequency band (200–300 Hz). To verify the sprocket's impact on noise, a cross-replacement test was designed: installing the same oil pump from a vehicle without abnormal noise significantly reduced the thumping sound. Upon reinstalling the original oil pump, the noise intensity returned to its initial state. Preliminary analysis identified the oil pump sprocket as the primary noise source. Subsequently, the oil pump from another vehicle exhibiting a pronounced knocking noise was transplanted into the test vehicle. The knocking noise intensity became more pronounced than in the original vehicle, definitively confirming the oil pump sprocket as the core source of this noise [16]. As shown in Figure 3, the spectrogram of abnormal parts shows significant energy at 300 Hz compared to normal parts.

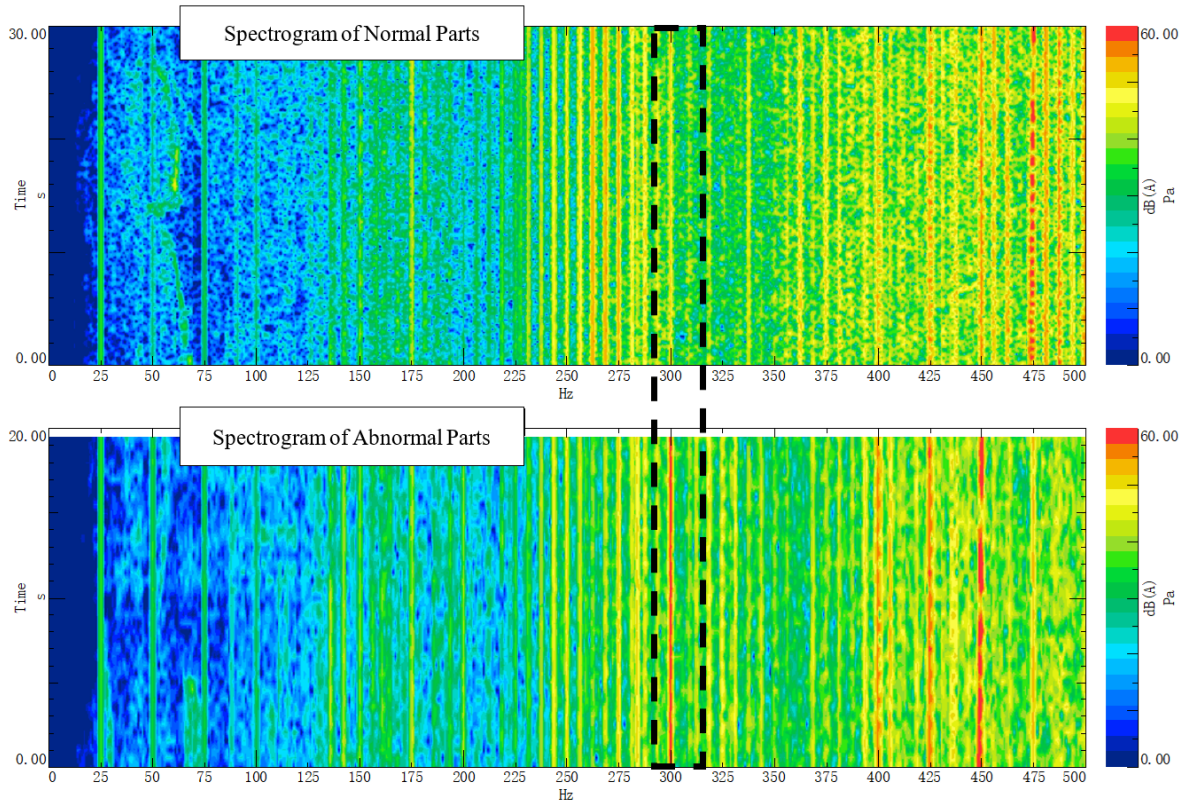

Figure 3. Spectrogram of Normal Parts vs. Abnormal Parts (Abnormal parts show significant energy at 300 Hz).

2.4. Differential Analysis of Abnormal-Sounding Components

Comparing the dimensions and performance of abnormal-sounding components with normal oil pump components revealed significant differences in the tooth flank chamfer dimensions of the sprockets (as shown in Figure 4). The specific findings are as follows (as shown in Table 2):

(1) Tooth Flank Chamfer Dimension: The measured chamfer dimension on abnormal parts was 0.58 mm, while all normal parts measured above 0.66 mm (including 1 normal part without abnormal noise and 5 production-inspected parts). The drawing specification requires 0.7 ± 0.2 mm, indicating that the abnormal parts' actual measurement falls below the lower limit.

(2) Synchronous comparison with counterpart design specifications reveals that the counterpart crankshaft sprocket tooth flank chamfer design requirement is 0.8 ± 0.2 mm. The abnormal-sounding parts exceed this design requirement.

Analysis of measured data and technical design requirements indicates that the tooth flank chamfer dimension of the oil pump sprocket is a critical factor in the knocking noise. Theoretical calculations and finite element simulation analysis were first conducted to systematically investigate the influence mechanism of this chamfer dimension on the knocking noise [17].

Table 2. Sprocket Measurement Data.

Inspection Items	Production Spot-Checked Samples					1# Abnormal	2# Normal
S1 tooth profile runout	1#	2#	3#	4#	5#	0.01	0.06
Size 0 (0/−0.25)	−0.13	−0.01	−0.06	−0.01	−0.01	−0.1	−0.13
Arc surface R8.5 ± 0.5	8.75	8.64	8.62	8.59	8.7	8.92	8.85
Size 0.7 ± 0.2	0.68	0.66	0.68	0.68	0.7	0.58	0.67
S2 tooth profile runout	0.05	0.03	0.05	0.05	0.05	0.05	0.04
Size 0 (0/−0.25)	−0.01	−0.01	−0.01	−0.01	−0.01	−0.01	−0.01
Arc surface R8.5 ± 0.5	8.54	8.48	8.5	8.5	8.49	8.51	8.52
Size 0.7 ± 0.2	0.65	0.67	0.65	0.67	0.68	0.59	0.66

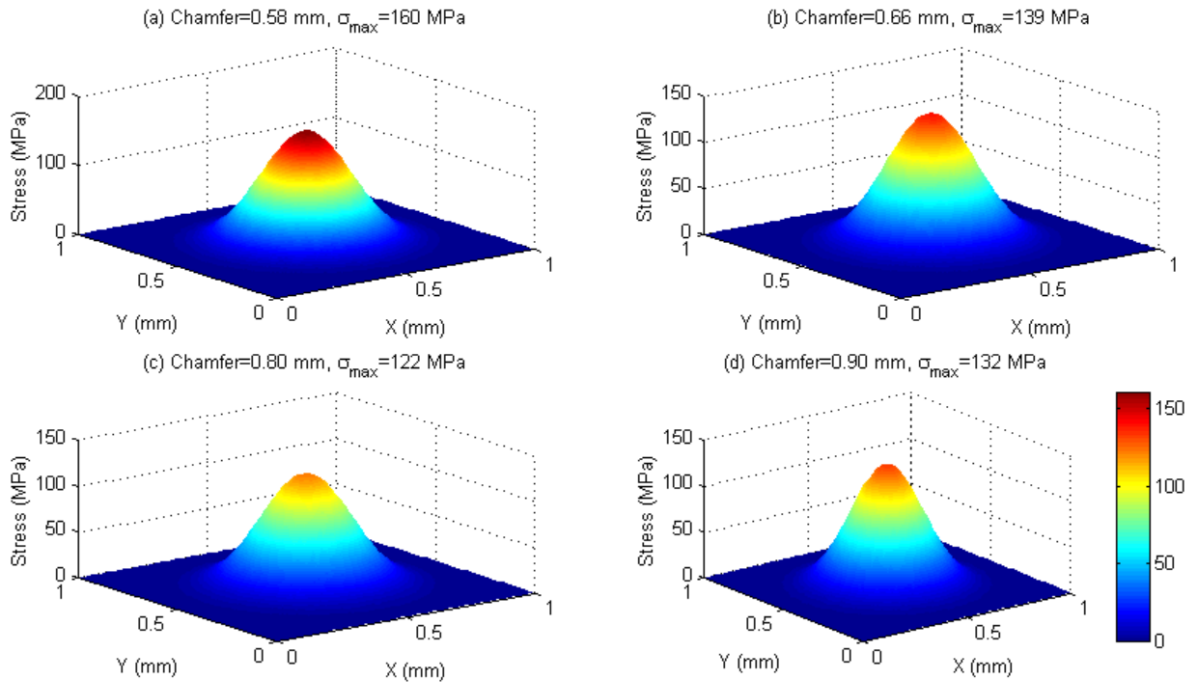

Figure 4. Finite Element Simulation.

3. Theoretical Analysis of Flank Chamfers on Meshing Impact Forces

3.1. Impact Force Model Based on Hertzian Contact Theory

The meshing process between sprockets and chains can be simplified as an elastic contact problem. According to Hertz's contact theory, the relationship between the contact stress amplitude and the contact curvature radius is:

$$\sigma_{\max} = \frac{3F}{2\pi a^2}, a = \sqrt[3]{\frac{3FR}{4E^*}} \tag{1}$$

In the equation, $\sigma_{\max}$ denotes the contact stress amplitude, F represents the impact force, a is the contact area, R is the contact curvature radius, and E^* is the equivalent elastic modulus.

Reducing the chamfer dimension, such as from 0.66 to 0.58, leads to a decrease in the contact curvature radius R and a reduction in the contact area a, resulting in an increase in the maximum contact stress. Finite element simulations conducted with relevant sprocket and chain parameters revealed that the peak contact stress reached 160 MPa when the chamfer was 0.58, decreased to 139 MPa at 0.66, and achieved the lowest value of 122 MPa at 0.8 (as shown in Figure 4) [18].

3.2. Impact Energy and Vibration Excitation

The Fourier transform of the time-domain signal $F(t)$ for the meshing impact force is:

$$F(\omega) = \int_{-\infty}^{\infty} F\ （t）\ e^{-jwt} dt \tag{2}$$

(1) The impact force pulse of the 0.58 chamfered specimen exhibits a narrow pulse width and high amplitude, with its spectrum showing concentrated energy at 300 Hz (Figure 5a);
(2) The impact energy of the 0.66 chamfered specimen spreads toward lower frequencies, with the 300 Hz component attenuating (Figure 5b).

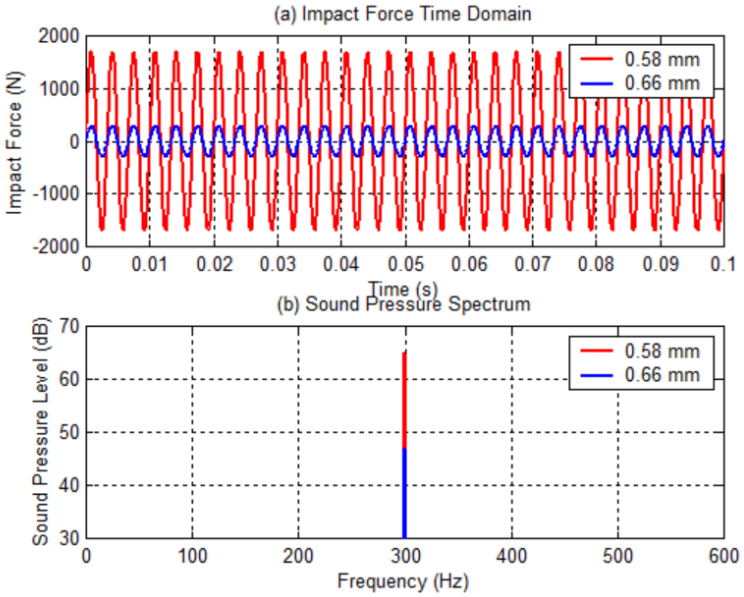

Figure 5. (a) Time-Domain Impact Force Waveform and (**b**) Normalized Sound Pressure Spectrum

4. System Resonance and Noise Coupling Mechanism

Resonance Frequency Response Analysis

When the meshing impact frequency f = 24 × 750/6 = 300 Hz couples with the crankshaft's half-order rotational excitation (6.25 Hz), the system resonates. The impact energy of the 0.58 chamfered sample is amplified in the 300 Hz frequency band, with NVH testing showing a sound pressure level reaching 65 dB. For the 0.66 chamfered sample, energy attenuation reduces the 300 Hz sound pressure level to 47 dB. Key dimensional parameters of the input sprocket and chain were analyzed via MATLAB simulation. Results indicate that a tooth flank chamfer of 0.80 achieves the lowest 300 Hz sound pressure level at 43 dB, as shown in Figure 6 [19].

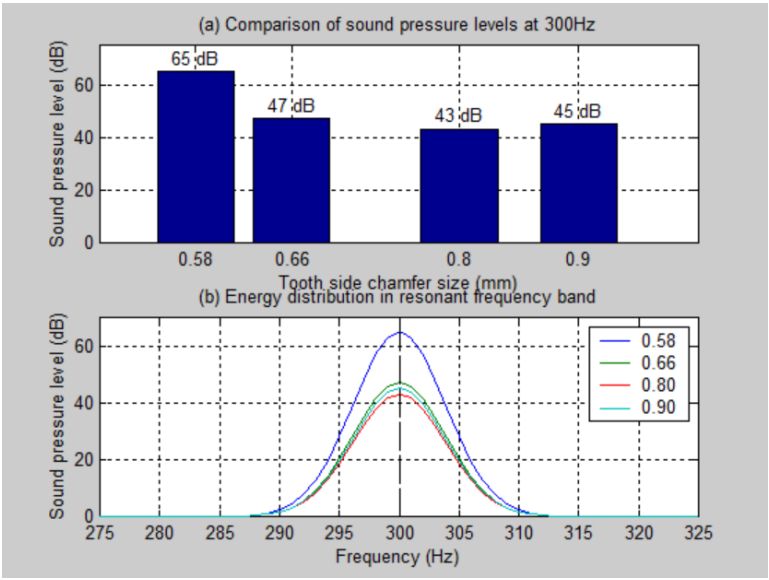

Figure 6. Comparison of Sound Pressure Levels for Different Chamfer Sizes.

5. Experimental Validation

5.1. Verification of Sprocket Tooth Flank Chamfer Dimensions

To further validate the accuracy of the aforementioned theoretical analysis, six sets of samples were prepared by grouping according to chamfer dimensions (lower limit 0.5 mm, median 0.7 mm, upper limit 0.9 mm) for in-vehicle testing (as shown in Table 3). Results indicate: Specimens with the lower limit (0.5 mm) exhibited higher noise intensity accompanied by pronounced knocking sounds; specimens with the mid-range value (0.7 mm)

showed significantly reduced noise intensity and were evaluated as acceptable by the NVH specialist team; specimens with the upper limit (0.9 mm) demonstrated markedly lower noise intensity than the mid-range specimens, with abnormal noise characteristics eliminated and performance exceeding design requirements.

Table 3. Results for Tooth Profile Dimensions and Flank Chamfers.

Serial Number	Tooth Flank Chamfer Dimensions	Group Evaluation Results
1	0.92 (upper limit component)	Not apparent (superior to the median component)
2	0.66 (Median component)	Not apparent
3	0.66 (Median component)	Not apparent
4	0.52 (lower limit component)	apparent
5	0.54 (lower limit component)	apparent
6	0.52 (lower limit component)	apparent
7	0.57 (Noise-generating component)	apparent
8	0.58 (Noise-generating component)	apparent

5.2. Small-Batch Trial Assembly Verification

Based on the optimized solution, sprockets with adjusted tooth flank chamfer dimensions to 0.8 ± 0.1 mm (balancing machinability and noise reduction requirements) underwent small-batch trial assembly (50 units total). Testing and evaluation by the NVH team confirmed that the trial samples exhibited no noticeable knocking sounds, with significantly reduced noise compared to the original vehicle state, validating the engineering effectiveness of the dimensional optimization [20].

6. Tolerance Zone Optimization

Tooth Profile Chamfer Tolerance Optimization

The original design of 0.7 ± 0.2 mm posed a risk of reaching the lower limit. Engineering optimization adjusted it to 0.8 ± 0.1 mm. Monte Carlo simulation validation confirmed that the optimized tolerance reduces NVH failure rate from 15% to 0.1%.

7. Conclusions

Mechanical meshing noise originates from key geometric parameters, such as chamfers, through chained transmission via the multiphysics coupling pathway of “contact stress-impact energy-resonance response”. Research indicates that the modulation effect of low-frequency excitation (e.g., half-order vibrations) with mid-to-low-frequency structural resonance is a common mechanism for noise generation. Optimizing key geometric parameters can systematically reduce impact energy density, thereby suppressing resonance responses and enhancing NVH performance. Specifically, this research identifies the tooth flank chamfer dimensions as a critical geometric parameter. The optimization direction for designers is to shift the tolerance band upward to avoid the lower design limit. For the engine oil pump sprocket studied here, a chamfer specification of 0.8 ± 0.1 mm was validated to be optimal. Furthermore, the design principle of specifying chamfer dimensions that ensure a contact curvature radius sufficient to minimize peak contact stress under operational loads is a universal guideline for transmission components. This conclusion provides universal design principles for noise control in transmission components. Implementing coordinated optimization of key parameters along the energy transfer chain enables end-to-end noise reduction from source to propagation path.

Author Contributions: Q.Z.: methodology, data curation, writing, reviewing, and editing; J.L.: Conceptualization; X.Z.: supervision; W.Z.: writing—original draft preparation; B.Z.: visualization; data curation; S.L.: investigation, validation. All authors have read and agreed to the published version of the manuscript.

Funding: This research received no external funding.

Institutional Review Board Statement: Not applicable.

Informed Consent Statement: Not applicable.

Data Availability Statement: Not applicable.

Conflicts of Interest: The authors declare no conflict of interest.

Use of AI and AI-Assisted Technologies: No AI tools were utilized for this paper.

References

1. Troedsson, I.; Vedmar, L. A Dynamic Analysis of the Oscillations in a Chain Drive. *J. Mech. Des.* **2001**, *123*, 395–401.
2. Johnson, K.L. Contact Mechanics; Cambridge University Press: Cambridge, UK, 1985.
3. Calì, M.; Sequenzia, G.; Oliveri, S. M.; Fatuzzo, G. Meshing Angles Evaluation of Silent Chain Drive by Numerical Analysis and Experimental Test. *Meccanica* **2016**, *51*, 475–489.
4. Bucknor, N.K.; Freudenstein, F. Kinematic and Static Force Analysis of Rocker-Pin Jointed Silent Chains with Involute Sprockets. *J. Mech. Des.* **1994**, *116*, 842–848.
5. Mahalingam, S.; Bishop, R.E.D. The Response of a System with Repeated Natural Frequencies to Force and Displacement Excitation. *J. Sound Vib.* **1974**, *36*, 285–295.
6. Zhan, P.; Qiang, Y.; Jiang, Z. Y.; Wei, L. J. Study on Mechanism and Suppression Method of Flow-Induced Noise in High-Speed Gear Pump. *Arch. Acoust.* **2024**, *49*, 49–60. https://doi.org/10.24425/aoa.2023.146824
7. Tang, C.; Wang, Y. S.; Gao, J. H.; Guo, H. Fluid-sound coupling simulation and experimental validation for noise characteristics of a variable displacement external gear pump. *Noise Control Eng. J.* **2014**, *62*, 123–131. https://doi.org/10.3397/1/376212
8. Ferrari, C.; Morselli, S.; Miccoli, G.; Hamiche, K. Integrated CFD-FEM approach for external gear pump vibroacoustic field prediction. *Front. Mech. Eng.* 2024, 10, 1298260. https://doi.org/10.3389/fmech.2024.1298260
9. Hu, W.; Li, H.; Zhuang, J. Non-Asbestos Fiber Gasket Materials & Their Applications in Automobile Powertrain Sealing. *Int. J. Automot. Manuf. Mater.* **2024**, *3*, 5. https://doi.org/10.53941/ijamm.2024.100011
10. Chen, M.; Xu, C.; Li, J.; Zhao, W.; Li, P.; Chen, Z.; Zhang, J.; Zhang, L. Exhaust Noise Optimization of Gas Engine Aftertreatment. *Int. J. Automot. Manuf. Mater.* **2026**. https://doi.org/10.53941/ijamm.2026.100008
11. Foraste Gomez, L.; Aihara, R.; Chen, Y.; Pan, F.; Nowaczyk, K. A Multi-Physics Approach to Predict High-Frequency NVH and Nonlinear Modulation in Oil Pump Drives. In Proceedings of Noise and Vibration Conference & Exhibition, Grand Rapids, MI, USA, 7 September 2021. https://doi.org/10.4271/2021-01-1099
12. Wang, Z.; Hu, Z.; Tian, Z.; Chen, S. Dynamic performance analysis of a gear transmission system due to cavitation in gerotor pump. *J. Low Freq. Noise Vibr. Act. Control* **2024***, 43*, 651–668. https://doi.org/10.1177/14613484231216232
13. Huang, F.; Zeng, X.; Wang, X.; Qiao, X.; Wang, Y.; Fang, L.; Zhang, Y.; Liu, D.; Deng, Y. Research on Abnormal Starting Noise of Efficient Engine Caused by Abnormal Combustion Noise. *Int. J. Automot. Manuf. Mater.* **2024**, *3*, 1. https://doi.org/10.53941/ijamm.2024.100007
14. Li, D.; Rong, L.; Mao, N.; Song, Y.; Liang, R.; You, J. Simulation of Vibration Characteristics of the Front MacPherson Suspension of a Sightseeing Vehicle. *Int. J. Automot. Manuf. Mater.* **2024**, *3*, 1. https://doi.org/10.53941/ijamm.2024.100019
15. Jin, Y.; Zhao, T. Analysis and Improvement of In-Cabin Acoustic Quality Issues Caused by Engine Half-Order Vibrations. *Automot. Eng.* **2020**, *42*, 396–400. https://link.cnki.net/doi/10.19562/j.chinasae.qcgc.2020.03.017. (In Chinese)
16. Zhou, Z.; Liu, F.; Pan, W. Research and Optimization on Objective Evaluation Method of Transmission Oil Pump Noise. *Chin. J. Automot. Eng.* **2025**, *15*, 151–158. https://doi.org/10.16638/j.cnki.1671-7988.2025.020.015. (In Chinese)
17. Chen, Z.; He, P. Rolling Bearing Fault Diagnosis Considering Long-Term Dependence and Time-Frequency Feature Fusion. *Int. J. Automot. Manuf. Mater.* **2025**, *4*, 4. https://doi.org/10.53941/ijamm.2025.100016
18. Veikos, N.M.; Freudenstein, F. On the Dynamic Analysis of Roller Chain Drives: Part I—Theory. *Mech. Mach. Theory* **1992**, *27*, 225–237.
19. Pedersen, S.L.; Hansen, J.M.; Ambrósio, J.A.C. A Roller Chain Drive Model Including Contact with Guide-Bars. *Multibody Syst. Dyn*. **2004**, *12*, 285–301.
20. Ye, J.; Yong, Y. Design and Development of a Dual-Cavity Oil Pan for an Engine. *Int. J. Automot. Manuf. Mater.* **2026**, *5*, 4. https://doi.org/10.53941/ijamm.2026.100003